

High-Pressure Reactivity of Model Hydrocarbons Driven by Near-UV Photodissociation of Water

Matteo Ceppatelli,^{†,‡} Roberto Bini,^{*,‡} and Vincenzo Schettino^{†,‡}

LENS, European Laboratory for Nonlinear Spectroscopy, Via N. Carrara 1, I-50019 Sesto Fiorentino, Firenze, Italy, and Dipartimento di Chimica dell'Università di Firenze, Via della Lastruccia 3, I-50019 Sesto Fiorentino, Firenze, Italy

Received: July 24, 2009; Revised Manuscript Received: September 18, 2009

The ambient temperature photoinduced reactivity of mixtures containing water and some of the simplest model hydrocarbons has been studied in a diamond anvil cell below 1 GPa. The near-UV 350 nm emission of an Ar ion laser has been employed to photodissociate water molecules through two-photon absorption processes. The hydroxyl radicals generated through this process are able to trigger a chemical reaction in the mixtures containing ethane and acetylene, which are otherwise stable under the same P – T – $h\nu$ conditions, whereas the contribution of water has no effect or is very limited in the case of the ethylene and propene mixtures, respectively. The reaction evolution and the reaction products were characterized by using FTIR spectroscopy. The formation of fluorescent products limits or prevents, as in the case of acetylene, the characterization by Raman spectroscopy. Particularly relevant is the in situ efficient sequestration of the CO₂ formed during the reaction, through the formation of a clathrate hydrate, in the mixtures where water is largely in excess.

1. Introduction

The high-pressure reactivity of simple molecular systems is a well-established research field of remarkable interdisciplinary interest.¹ The efficient tuning of the intermolecular distances realized through the increase of pressure causes a progressive change of the molecular electronic density distribution that is able to trigger a chemical reaction between nearest neighbor molecules. The pressures required for such spontaneous transformations range from a few gigapascals, for the smaller unsaturated hydrocarbons,^{2–6} to tens of gigapascals in the case of nitrogen^{7–9} or carbon dioxide.^{10,11} Extended materials are generally obtained from all these reactions, but the reactivity of unsaturated hydrocarbons is particularly relevant for the possibility to synthesize polymeric materials recoverable at ambient conditions. Nevertheless, the pressure required for the spontaneous transformations are too high to be of interest for large-volume syntheses, which are generally carried out below 1 GPa. Therefore, to make these processes appealing for applicative purposes, it is necessary to scale down the reaction pressure. In addition, it should be mentioned that also in this low-pressure range most of the simplest molecules are generally solid. The constraints posed by the crystal structure can considerably increase the activation energy of the reaction with respect to the fluid phases, where the energetic barriers for the internal and external molecular motions are generally lower. Nevertheless, the lower density of the fluid does not allow the realization of the critical distances for the occurrence of the reaction.

In high-density compressed fluids, it is possible to trigger a chemical reaction by exploiting the structural and charge density distribution changes produced by an electronic transition. The excited molecule is in fact generally characterized by a stretching

of the bonds, a lowering of rotational and torsional barriers, and an increase of the polarity. In some cases, even dissociation, ionization, or excimers formation can take place, originating chemically aggressive species.¹² Laser light has been successfully employed in several cases to lower the onset of a high-pressure reaction by using excited molecules generated through two-photon electronic absorption processes.¹³ By this approach the threshold pressure can be lowered also by 1 order of magnitude, as in the ethylene case,⁵ making the corresponding syntheses accessible to large-volume applications. In addition, remarkable results in terms of selectivity and yields of the photoactivated processes have been obtained.⁵ As a final consideration, photoexcitation and moderate pressure conditions are encountered in natural environments and events, extending the interest for this kind of molecular reactivity to bioscience, space, and environmental chemistry.

This approach can be also useful to activate high-pressure chemical reactions in very stable systems by using photoactivated initiators. Recently, the hydroxyl radicals, produced in the photodissociation of water molecules by near-ultraviolet radiation at room temperature and pressures of a few tenths of a gigapascal, have been successfully employed to trigger chemical reactions in mixtures of water with carbon monoxide or nitrogen.¹⁴ Besides the interest for the synthesis of specific products like hydrogen, these studies are mandatory to understand the mechanisms and the dynamics of the formation of specific molecular compounds in the space and on the surfaces of planets and comets. Water is indeed one of the most abundant polyatomic molecule on the Earth's surface and in the cosmos,¹⁵ and its photodissociation is the primary step in many chemical reactions occurring in the Earth's atmosphere, planets, comets, or other space environments. For example, photoreactions in gas mixtures have been studied to investigate the photochemical abiotic formation of bioorganic compounds¹⁶ or to explain the presence of methane in the Martian atmosphere.¹⁷ Also mixed ices of different composition have been studied to understand

* Corresponding author. E-mail: bini@chim.unifi.it.

[†] LENS, European Laboratory for Nonlinear Spectroscopy.

[‡] Università di Firenze.

the chemical processes activated by the solar irradiation occurring at the planets surface.^{18,19} The efficiency of the photoinduced reactivity of the water molecule originates from the dissociative character of all its excited states. The absorption of high-energy photons ($\lambda < 185$ nm) gives rise to single and multiple ionizations with the formation of neutral and ionic fragments, either in the ground or in the excited states, able to trigger many chemical reactions. Evidence for the formation of OH radicals and H atoms has been reported both in one-photon (184.9 nm)²⁰ and two-photon absorption experiments (281–286 nm).²¹ The latter results are of interest because they indicate the possibility of using lower energy photons to generate radicals through multiphoton absorption processes.

In this framework, the study of binary systems composed by water and simple hydrocarbons is particularly relevant because of their not unusual presence in nature.²² The basic idea of our research is that, at the high-density conditions achievable by the application of suitable pressures, the time scale for the recombination of the radicals produced by the photodissociation of the water molecules becomes comparable to the mean free time relative to the collisions with the surrounding molecules. Therefore, the radicals produced have a significant probability of reacting with a neighbor hydrocarbon molecule. Ethane, ethylene, and acetylene were chosen because they are the simplest molecules containing a single, double, and triple C–C bond, respectively, thus representing model systems for the reactivity of more complex molecules. We have studied also the propene/water mixture where two different types of C–C bond are present. In addition, with the only exception of ethane, the reactivity under pressure of these systems is well-established.^{2,3,6,23–25}

2. Experimental Section

A membrane diamond anvil cell (MDAC) equipped with Ila type diamonds was employed to pressurize the mixtures. Both stainless steel and rhenium gaskets with diameters ranging between 150 and 200 μm and thickness of about 45 μm were employed to contain the samples. The mixtures were loaded by separately condensing H₂O and the hydrocarbons (purity $\geq 99.99\%$) onto the diamonds while the cell was mounted on the cold tip of a close-cycle cryostat. The deposition was realized through a capillary, placed at about 2 mm from the diamonds tips, connected through a flange to a deposition line that was pumped several hours before starting the cooling of the cell. Water was condensed below 120 K by using helium as gas carrier. The hydrocarbons were then condensed when the temperature reached about 30 K. The deposition steps could be followed by visual observation through a microscope and the relative amounts could be roughly adjusted. Once the sample region was completely covered by the crystalline sample, the cell was screwed and helium pressure applied in the membrane to seal the sample. The temperature was then raised up to ambient temperature by keeping the membrane pressure constant. Infrared and Raman spectra were employed to check the sample purity. The pressure was measured by the ruby fluorescence method.

The high-pressure reactions were triggered by focusing the UV multiline emission of an Ar ion laser (350 nm) onto the sample, taking care to homogeneously irradiate the whole sample. FTIR absorption measurements were performed with a Bruker-IFS 120 HR spectrometer modified for high-pressure measurements.^{26,27} The instrumental resolution was 1 cm^{-1} . Raman spectra were measured in a back-scattering geometry by using the 647.1 and 752.5 nm lines of a Kr⁺ laser. The

scattered light was dispersed by a single stage monochromator (900 grooves/mm) and analyzed by a CCD detector with a resulting instrumental resolution of 0.7 cm^{-1} .

The stability of the mixtures at high pressure was carefully checked by keeping the sample at the desired pressure for the experiment for a few days (2–5) before performing the irradiation cycles. The FTIR spectra recorded before, during, and after this period did not show any change. Possible interactions between water and gasket were also checked by leaving the water for some days in the cell and, finally, by irradiating the sample under the same duration and laser power conditions employed for the mixtures. Finally, we used both rhenium and stainless steel as gasket materials without observing any difference in the reactions evolution.

3. Background

The absorption spectrum of water consists of broad absorption bands starting approximately below 200 nm.²⁸ Recently, synchrotron radiation has been employed to analyze the lowest absorption bands between 6.0 and 11.0 eV.²⁹ Three bands centered at 7.447, 9.672, and 10.011 eV have been observed and assigned to the transitions from the $\tilde{X}(^1A_1)$ lowest neutral ground state to the $\tilde{A}(^1B_1)$, $\tilde{B}(^1A_1)$, and $\tilde{C}(^1B_1)$ states, respectively. A fourth band centered at 10.163 eV is due to excitation to the $\tilde{D}(^1A_1)$ state. The ionization energy threshold of H₂O is reported above 12 eV (see ref 29 and refs therein). The first absorption band is quite broad with the electronic origin located at 7.069 eV. This value is much higher than the origin reported in previous optical absorption experiments (6.0 eV) in the vacuum UV region.²⁸ The lowest excited state, $\tilde{A}(^1B_1)$, has been shown to be dissociative like all the other excited states of water. The direct excitation to this state (155–175 nm) gives rise to a dissociation proceeding on a single potential energy surface and producing a hydrogen atom and an hydroxyl radical in its electronic ground state ($^2\Pi$).³⁰ Excitation with lower wavelength radiation gives access to higher energy states opening new paths for dissociation through conical intersections, leading to collinear molecular geometries.³¹ For example, the excitation to the $\tilde{B}(^1A_1)$ state, besides ground-state hydroxyl radicals, produces also small amounts of excited OH ($^2\Sigma$), H₂ and O species.³² Transitions from the totally symmetric ground state to all the excited states are two-photon allowed.

In our experiments, we have employed the 350 nm (3.54 eV) emission line of an Ar⁺ laser to excite the lowest electronic excited state through the symmetry allowed $\tilde{X}(^1A_1) \rightarrow \tilde{A}(^1B_1)$ two-photon transition.

4. Results

4.1. Ethylene Mixture. Ethylene in the monoclinic crystal structure ($P2_1/n$, $Z = 2$) spontaneously polymerizes once compressed above 3 GPa at ambient temperature.^{23,24} The same reaction can be triggered at a few tenths of a gigapascal by irradiating fluid ethylene with laser wavelengths shorter than 488 nm.⁶

After the loading, at pressure below 1 GPa, the C₂H₄/H₂O mixture appears as a biphasic fluid system. A comparable amount of the two mixture components is estimated by comparing the IR spectra of the pure components with that of the mixture. The considerable amount of water is revealed by the out-of-scale O–H stretching band (see Figure 1), centered at 3250 cm^{-1} , that hides the C–H stretching bands of ethylene and by the intensity of the absorption peak at 1650 cm^{-1} due to the bending mode. Also the amount of ethylene is remarkable

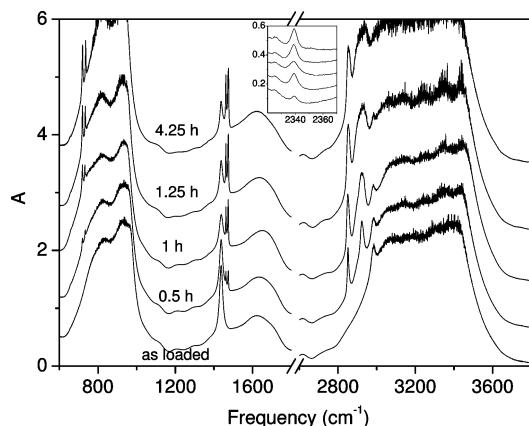


Figure 1. Evolution of the IR spectrum of the ethylene/water mixture after irradiation cycles performed with 200 mW of the 350 nm Ar ion laser line. The pressure slightly changed during the irradiation cycles ranging between 0.3 and 0.5 GPa during the whole experiment. For each spectrum the total irradiation time is reported. In the inset an enlarged view of the CO₂ antisymmetric stretching absorption region is shown.

as inferred by the intensities of the bands relative to the CH₂ wagging mode at about 950 cm⁻¹ and to the bending mode at 1440 cm⁻¹.

Short irradiation cycles of 15–30 min were performed by using 200 mW of the 350 nm Ar ion laser emission line. The sample pressure appreciably dropped after each irradiation cycle and it had to be compensated by raising the helium pressure in the membrane of the cell. For this reason, the irradiations were performed at pressures ranging between 0.3 and 0.5 GPa. After the first irradiation, about 30 min long, the characteristic bands of polyethylene are clearly visible in the spectra (see Figure 1). The two doublets at about 730 and 1460 cm⁻¹ correspond to the polyethylene crystal components (orthorhombic *Pnam*, *Z* = 2) of the rocking and of the scissoring modes, respectively. Below 3000 cm⁻¹ the stronger absorptions of the C–H stretching modes overlap to the low-frequency side of the out-of-scale absorption band of water. The amount of polymer increases after each irradiation cycle until the ethylene is almost completely consumed. In contrast, the absorption bands of water remain almost unaltered during the irradiations, thus suggesting that water does not participate in the photoinduced reaction. A very small amount of CO₂ forms after the first irradiation cycle, as revealed by the appearance of the antisymmetric stretching mode (see the inset in Figure 1), but this quantity negligibly increases on further irradiation.

The microphotograph of the sample collected after the last irradiation cycle, which shows a textured polymer sample, and the IR spectrum of the recovered polyethylene indicate the crystalline nature of the sample (see Figure 2). The reaction therefore proceeds with the same features reported for pure ethylene.⁶ This is not an obvious result considering, for example, the behavior of carbon monoxide that, in spite of its marked instability under irradiation, reacts to a large extent with water.¹⁴

4.2. Ethane Mixture. At room temperature, pure ethane crystallizes above 2.7 GPa.³³ Like several other small hydrocarbons,²² ethane also forms a hydrate clathrate that is stable above 0.1 GPa at ambient temperature.³³ After the loading the pressure in the cell at ambient temperature was about 0.6 GPa and, therefore, in these *P*–*T* conditions our sample should form a clathrate hydrate. The sample appears indeed heterogeneous (see Figure 3) with several crystals of different dimensions that occupy all the sample region. Besides the water bands, already

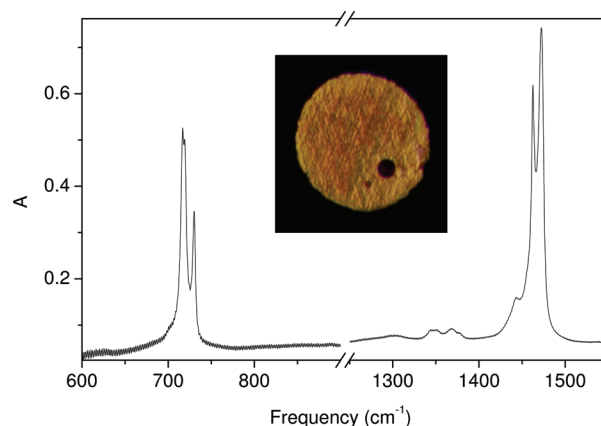


Figure 2. IR spectrum of the polyethylene recovered from the photoinduced reaction of the ethylene/water mixture. The photo of the polymeric sample has been taken before opening the cell once the pressure in the membrane was completely released.

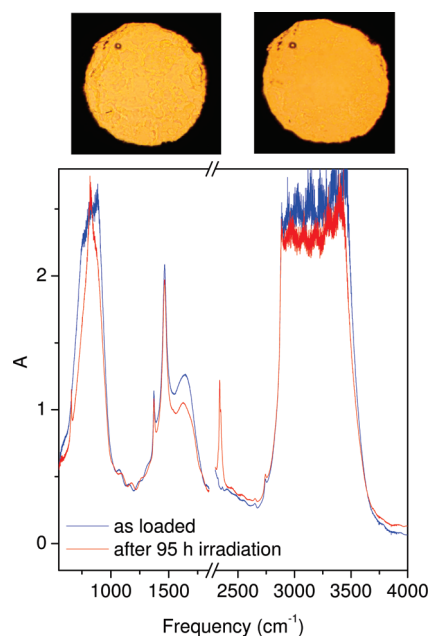


Figure 3. Monitoring the effects of the irradiation cycles (350 nm, 100–600 mW) on the ethane/water mixture at 0.6 GPa. The microphotographs collected before (left) and after (right) all the irradiation cycles are shown together with the corresponding IR absorption spectra.

described in the ethylene section, the IR absorption spectrum (see Figure 3) shows, a band at 1469 cm⁻¹, due to the CH₃ deformation of ethane. This is the only vibrational band of ethane that can be clearly distinguished, whereas the C–H stretching and rocking modes, at 2985 and 822 cm⁻¹, respectively, are hidden or overlapped to the strong water bands. The sample was irradiated (350 nm) at this pressure with increasing laser power ranging from 100 to 600 mW. As shown in Figure 3, while the sample appearance does not appreciably change even after several hours of irradiation, but the occurrence of a chemical reaction is revealed by the FTIR spectra. In Figure 3 the IR spectrum measured after several irradiation cycles, about 95 h in total, is also reported. The reaction can be revealed by the appearance of the two bands at 670 and 2340 cm⁻¹ that are unambiguously assigned to the bending and antisymmetric stretching modes of CO₂, respectively. In spite of the very long irradiation, the extent of the reaction is extremely limited and seems to affect differently the ethane and water bands. The band

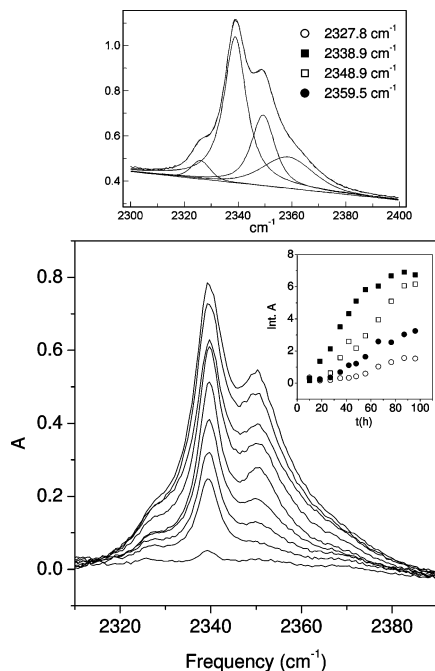


Figure 4. Evolution of the antisymmetric stretching absorption of CO₂ upon irradiation of the ethane/water mixture with the 350 nm laser line at 0.6 GPa (lower panel). The FTIR spectra have been collected, in order of increasing absorption, after successive irradiation cycles of 0.3 h, 800 mW; 8.3 h, 550 mW; 8.5 h, 650 mW; 8.2 h, 550 mW; 14 h, 650 mW; 7.5 h, 250 mW; 10.3 h, 250 mW; 8 h, 230 mW; and 9.3 h, 230 mW. The evolution of the integrated absorption of the four bands obtained by the deconvolution analysis (see upper panel) are reported in the inset as a function of the irradiation time.

relative to the bending mode of water, the only one in scale, shows an appreciable weakening, whereas the ethane band at 1469 cm⁻¹ is almost unaltered.

Looking in detail at the absorption of the antisymmetric mode of CO₂ (see Figure 4), we observe a rather complex structured profile that can be reproduced by the convolution of four peaks having maxima at about 2328, 2339, 2349, and 2359 cm⁻¹. All the peaks intensify with the irradiation time, thus allowing their assignment to the CO₂ formed during the photoinduced reaction. The frequencies of the two central peaks nicely agree with those measured in the type-I structure of carbon dioxide clathrate hydrate and correspond to the CO₂ occupation of large (2339 cm⁻¹) and small (2349 cm⁻¹) cages, respectively.^{34,35} Nevertheless, their intensity ratio differs, especially for long irradiation time, from the 3:1 ideal ratio expected for this structure. In the type-II structure, all the CO₂ molecules occupy the small cages and only the band at 2349 cm⁻¹ is observed.³⁴ Therefore, in the present case both structures likely form, giving rise to an intensity ratio lower than that expected for the pure type-I structure. This occurrence is also reported for clathrates of carbon dioxide contained in natural quartz samples, where both clathrate structures were detected.³⁶ In addition, Prasad and co-workers also observed a high-frequency broad band corresponding to the band peaked at 2359 cm⁻¹ observed in our spectra (see Figure 4). The shape and the position of this band is consistent with the formation of CO₂ clusters.^{37,38} Finally, a systematic ATR-IR study of the possible aggregation states of carbon dioxide in H₂O/CO₂ mixtures indicates that the last weaker peak at 2328 cm⁻¹ has to be assigned to liquid CO₂, which presents at ambient pressure and 223 K a broad band centered at 2325 cm⁻¹.³⁵

4.3. Propene Mixture. The pressure-induced reaction in propene has been investigated both experimentally²⁵ and by ab

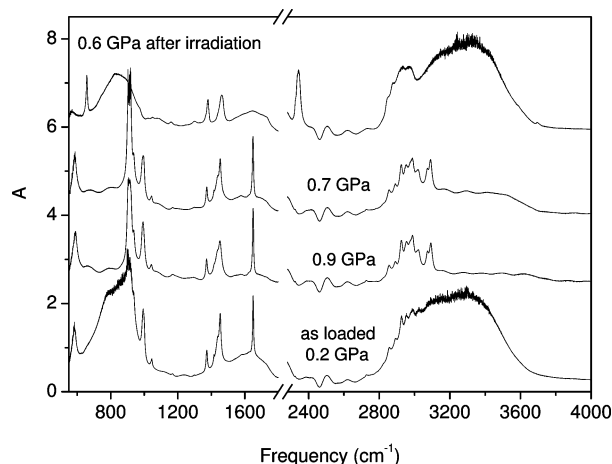


Figure 5. IR spectra of the propene/water mixture measured before (three lower traces) and after (top trace) irradiation for 8 h with 260 mW of the 350 nm laser line.

initio molecular-dynamics studies.³⁹ The reaction only occurs in the fluid phase, but not in the solid glassy phase, in spite of more drastic pressure conditions. This behavior was explained by the lack of long-range order in the solid and then with the absence of collective motions (lattice phonons) that modulate the interaction contacts among the molecules in the crystal. The role of the lattice phonons in triggering the solid-state reaction was invoked in several cases^{3,23,40} and has been recently demonstrated for crystalline benzene.⁴¹ The ambient temperature threshold for the occurrence of the purely pressure-induced reaction is about 2.5 GPa, but it is lowered to 0.75 GPa by using the 350 nm laser line to photochemically activate the reaction. In both cases, the product consists of a mixture of solid and liquid linear oligomers, but the amount of product is much larger in the photoinduced reaction.²⁵

The IR spectrum of the propene/water mixture measured at tenths of a gigapascal immediately after the loading is reported in Figure 5. The sharp bands of propene allow estimation of the relative amount of the components by comparing their absorbance with pure propene samples of comparable thickness. Also in this case we were able to produce a mixture composed of a comparable amount of propene and water. By increasing the pressure, the broad and strong bands of water seem to disappear. This behavior contrasts with our repeated observation, in the low-pressure regime (0.2–1.2 GPa), of an intensification of the O–H stretching water band with rising pressure, especially after crystallization. This peculiarity could be ascribed to a clathrate hydrate formation for which, to our knowledge, no data concerning the stability field are available. Lowering again the pressure to 0.7 GPa, the appearance of broad bands from water likely indicates the onset of the clathrate decomposition. The mixture was irradiated at this pressure with 260 mW of the 350 nm laser line. This is the same pressure where pure propene is reported to transform almost quantitatively once irradiated for 23 h with 500 mW of the same laser line.²⁵ In spite of the employment of half of the power, the propene completely reacts after only 8 h of irradiation, as revealed by Figure 5, where all the propene bands vanish after the irradiation cycle. In addition to the formation of carbon dioxide, revealed by both the bending and antisymmetric stretching modes, it is interesting to notice the reappearance of the strong water bands likely due to the clathrate destruction.

Once the pressure is released and the cell opened, a small amount of a dark red solid remains on the diamonds. The IR

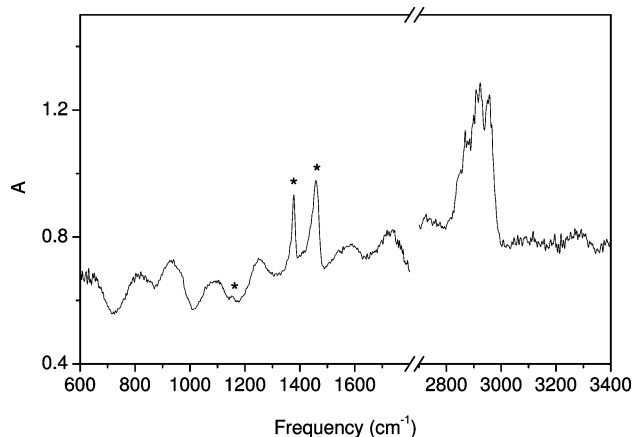


Figure 6. IR spectrum of the recovered solid material from the photoinduced reaction of the propene/water mixture. Asterisks indicate the bands that dominate the low-frequency spectrum of the recovered material both in the photoinduced and in the purely pressure induced reaction of pure propene.²⁵

spectrum of this material, reported in Figure 6, closely resembles that measured after the reaction in pure propene and assigned to small propene oligomers.²⁵ The C–H stretching region unambiguously indicates a saturated compound, but this result contrasts with the coloration of the sample, which could suggest a conjugated material, and with the strong sample fluorescence, which prevented the measurement of Raman spectra. In the pressure-induced polymerization of acetylene, the red coloration of the polyacetylene forming during the reaction was observable before any indication of the occurrence of the chemical reaction could be detected from the IR spectra.³ Here, a small amount of conjugated products is likely sufficient to color the sample, but it is not enough to be detected by IR spectroscopy.

4.4. Acetylene Mixture. The acetylene reactivity under pressure has been extensively studied either experimentally by Raman,² IR,^{3,42} and UV–vis absorption⁴³ spectroscopy or theoretically by ab initio simulations.^{44,45} The reaction is observed in the orthorhombic phase around 3.0 GPa, where a consistent volume reduction of the sample is accompanied by a deep red coloration.³ The spectroscopic detection of the characteristic Raman and IR bands of polyacetylene reveals the polymerization process. A further pressure increase causes the branching of the chains and the sample decoloration for the conjugation loss.

After the mixture was loaded into the cell at low temperature, care was taken to warm up the sample to ambient temperature by maintaining the pressure below 1–2 GPa. Failure in this procedure can result in the activation of the spontaneous polymerization reaction of acetylene. The occurrence of the polymerization can be readily revealed by visual observation because of the red coloration assumed by the sample even before the polymer bands become detectable in the IR spectra. The pressure was set between 0.3 and 0.5 GPa in all the different experiments. At this pressure, both the components should be fluid, but a triplet is observed in the Raman spectra of the C–C stretching region (ν_2) of acetylene, where, on the contrary, a single peak is observed in pure acetylene at the same P – T conditions.⁴⁶ The triplet structure is observed also when the pressure is lowered down to 0.1 GPa, thus ruling out possible inaccuracies in the pressure calibration or a metastability of the cubic phase, because the melting pressure at ambient temperature is reported at 0.7 GPa.⁴⁶ Therefore, this observation likely indicates the formation of an acetylene clathrate hydrate, which has been studied only at ambient pressure and low temperature.^{47,48}

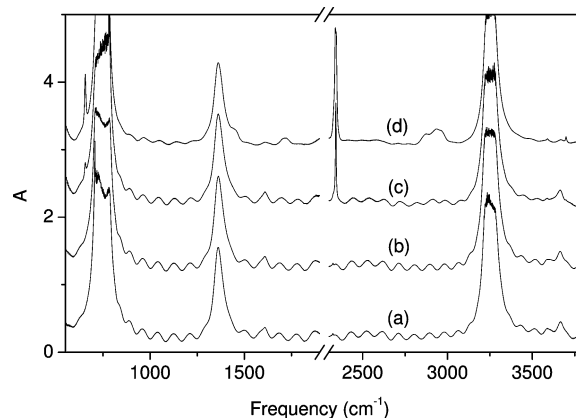


Figure 7. IR spectra measured in the acetylene-rich water mixture upon irradiation between 0.3 and 0.5 GPa: (a) before irradiation, (b) after 1.5 h of irradiation with 100 mW of the 457 nm laser line, (c) after 10 min of irradiation with 490 mW of the 350 nm laser line, and (d) after 1.5 h of irradiation with 490 mW of the 350 nm laser line.

We performed several experiments with different concentrations of the two components, but the significant outcome of the reaction can be highlighted by analyzing the mixtures in which one of the two components largely exceeds the other. The IR spectra showing the reaction evolution in the acetylene-rich mixture are reported in Figure 7. The three main absorptions are due to vibrational modes of acetylene: the antisymmetric C≡C–H bending (ν_5) mode at 747 cm^{-1} , the combination mode $\nu_4 + \nu_5$ at 1362 cm^{-1} , and the antisymmetric C–H stretching mode ν_3 at 3255 cm^{-1} . The two fundamental modes are saturated. Both the vibrational bands of water, the bending mode at 1609 cm^{-1} and the O–H stretching mode at 3665 cm^{-1} , are barely visible. In addition, the frequency and the shape of the O–H stretching mode indicate the presence of isolated or small clusters of water molecules. The irradiation with the 457 nm line of the Ar ion laser (1.5 h, 100 mW) does not produce any effects neither in the visual aspect of the sample nor in its IR spectrum. In contrast, a few minutes of irradiation with the 350 nm UV laser line gives rise to the sudden appearance of two sharp bands at 655 and 2342 cm^{-1} , assigned to the bending and antisymmetric stretching modes of CO_2 , respectively. Also, the sample appearance changes, showing a diffuse dark coloration. After one more irradiation cycle, the amount of CO_2 further increases, whereas the bands of water are not observable anymore. In addition, new bands are detected in the spectrum: a broad absorption between 2800 and 3015 cm^{-1} , another one at 1720 cm^{-1} , and a weak band at 1453 cm^{-1} appearing as a shoulder of the combination band of acetylene at 1362 cm^{-1} . All these bands belong to a solid product with a strong red coloration that can be recovered at ambient pressure. The IR spectrum of this product, measured at ambient pressure after the opening of the cell, is reported in Figure 8. The loss of the volatile products and of the unreacted acetylene allows the detection of another band at 1376 cm^{-1} that was covered by the stronger absorption due to the combination band of acetylene at 1362 cm^{-1} . In addition, the band at 1720 cm^{-1} presents a shoulder at 1730 cm^{-1} , whereas the high-frequency (2800–3015 cm^{-1}), broad band reveals now a structured absorption profile. Weaker absorptions are also observable between 800 and 1250 cm^{-1} .

We performed other experiments with very similar relative concentration of the mixture components lowering the power and the duration of the irradiation cycles. Three hours of using 200 mW of the 350 nm laser line are necessary to totally

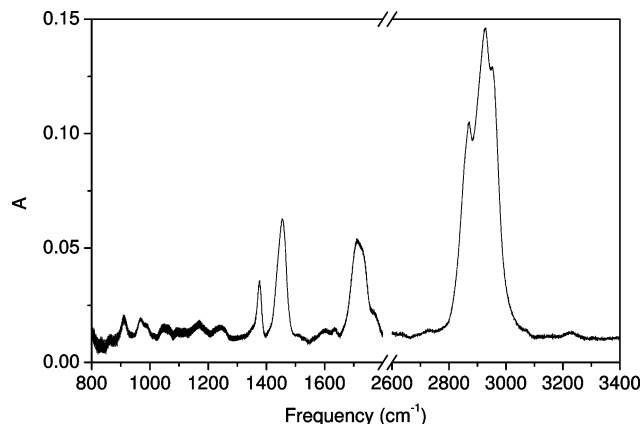


Figure 8. IR absorption spectrum of the solid material recovered from the photoinduced reaction in the acetylene-rich water mixture measured at ambient conditions after opening the cell. The interference fringes on the low-frequency side of the spectrum are due to reflections between the diamond surfaces.

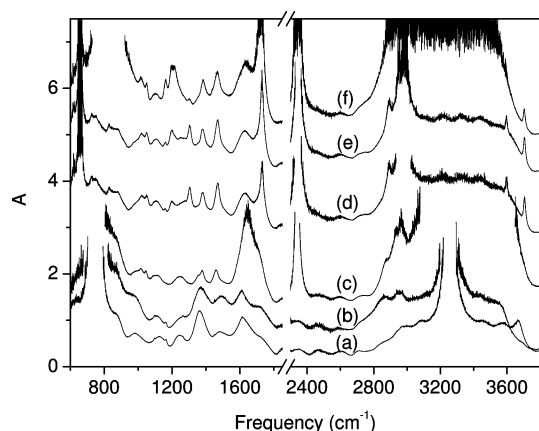


Figure 9. Evolution of the photoinduced reaction using the 350 nm laser line in an acetylene/water-rich mixture: (a) 0.1 GPa before irradiation, (b) 0.9 GPa before irradiation, (c) 0.2 GPa after 5 min of irradiation with 100 mW, (d) 1.1 GPa after a further irradiation of 4.25 h with 100 mW, (e) pressure lowered to 0.9 GPa after 40 h with respect to part d without any further irradiation, and (f) after 96 h with respect to part e at the same pressure and without any irradiation.

consume the water. The recovered product is exactly the same as that reported in Figure 8. In contrast, no changes in the IR spectrum as well as in the visual observation of the sample are detected when pure acetylene is irradiated for two hours with 440 mW of the 350 nm Ar⁺ laser line, firmly evidencing the role of water in triggering the chemical reaction.

The IR spectra describing the reaction evolution in a mixture where water is largely in excess are reported in Figure 9. Despite the laser power employed in this case being even lower (100 mW) than in the acetylene-rich mixture, the sample readily reacts after a few minutes of irradiation and the reaction proceeds until all the acetylene is consumed. Once the reaction starts, all the absorption bands of water greatly intensify, as already observed in the propene/water mixture. Also, in this case the most likely explanation is the destruction of the clathrate hydrate and the formation of liquid water. At the end of the irradiation cycles the reaction product is slightly different from that obtained in the acetylene-rich mixture for the presence of a band at 1306 cm⁻¹, which is characteristic of the methane molecule (antisymmetric bending). Furthermore, in this case the reaction evolves at constant pressure and temperature also while the sample is not irradiated (see spectra e, f in Figure 9), as shown by the disappearance of the methane bending peak at

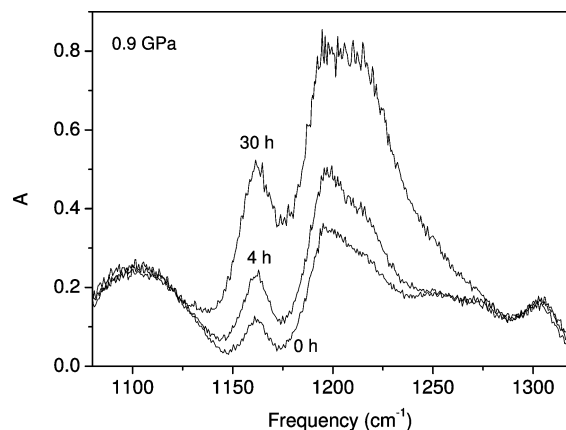


Figure 10. Time evolution of the C–O stretching region after the conclusion of the irradiation cycles (see spectra d, e, and f in Figure 9).

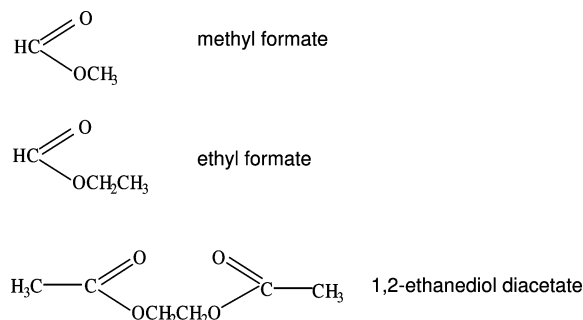


Figure 11. Compounds accounting for the IR spectrum of the product obtained from the high-pressure photoinduced reaction in acetylene/water-rich mixtures.

1306 cm⁻¹ and by the growth of the C=O (1730 cm⁻¹) and C–O (1207 cm⁻¹) stretching absorptions. The evolution with time of the C–O stretching absorption region is shown in Figure 10.

The assignment of the product absorption bands provides insight into its composition. The strong band at 1730 cm⁻¹ can be easily assigned to the carbonyl stretching mode, and its frequency is quite characteristic of formate esters.⁴⁹ The two bands of comparable intensity at 1468 and 1384 cm⁻¹ are from the asymmetric and symmetric CH₃ bending, respectively. The quite strong band at 1207 cm⁻¹, whose intensification as a function of time is reported in Figure 10, and the weaker band at 1163 cm⁻¹ nicely agree with the frequencies of the C–O stretching and CH₃ rocking modes of methyl formate, respectively. Weaker bands at 1018, 1050, and 1300 cm⁻¹ are not found in the spectrum of methyl formate, but the low-frequency doublet is found in the 1,2-ethanediol diacetate spectrum, whereas the 1300 cm⁻¹ band is observed in that of ethyl formate, all of them being characterized by a similar chemical composition (see Figure 11).

From stoichiometric considerations and by analogy with observations made in other systems,¹⁴ the huge amount of CO₂ produced in the reaction led us to suppose the formation of molecular hydrogen. Therefore, we monitored the reaction by Raman spectroscopy, but after few minutes of irradiation, the dark regions that formed in the sample (see Figure 12) gave rise to a strong fluorescence that prevented the Raman analysis, even when using the 752.5 nm emission of a Kr ion laser as the excitation line. Nevertheless, the IR spectra measured in this experiment provide an important insight about the evolution of the CO₂ formed during the reaction. In fact, the band shape

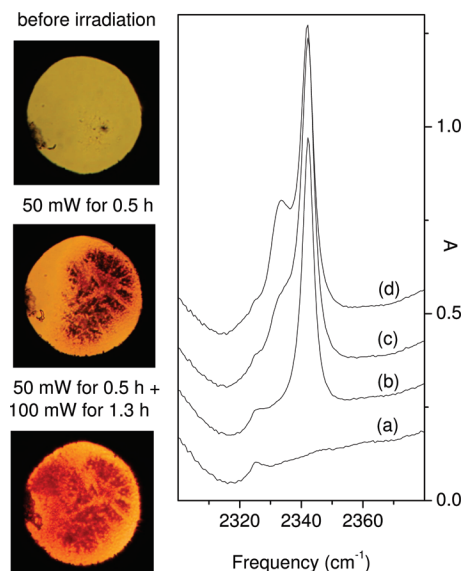


Figure 12. IR spectrum reporting the evolution of the CO₂ antisymmetric stretching absorption after short irradiation cycles of the acetylene/water mixture: (a) as loaded, (b) after 10 min of irradiation with 25 mW of the 350 nm laser line, (c) after an additional irradiation with 50 mW for 30 min, and (d) after an additional irradiation with 100 mW for 1.3 h. The microphotographs correspond, from top to bottom, to traces a, c, and d, respectively.

of the asymmetric stretching of CO₂ can be studied only after short irradiation cycles before the saturation of the corresponding absorption bands. The evolution of the asymmetric stretching of CO₂ is reported in Figure 12. The CO₂ formed after the initial irradiation cycle gives rise to a single band (2342 cm⁻¹) that can be assigned to carbon dioxide dissolved in water.³⁵ As the irradiation proceeds, a shoulder appears on the low-frequency side, intensifying on further irradiation, whereas the main peak weakens. This doublet has been already observed in the reaction of the ethane/water mixture and it was assigned to the formation of the carbon dioxide clathrate hydrate. Also, in this case such assignment seems to be the most reasonable, because the IR absorption of this mode in the type-I structure of the clathrate hydrate is characterized by a strong band at 2339.7 cm⁻¹ (ambient pressure and low-temperature conditions) and a weaker absorption at 2350.2 cm⁻¹.³⁴ Therefore, we can interpret the spectral evolution considering that at the beginning a small amount of carbon dioxide is dispersed as isolated molecules in the mixture, but as the concentration of CO₂ rises, the clathrate hydrate starts to form.

Ambient pressure chemical reactions induced by vacuum and extreme ultraviolet photoirradiation of acetylene/water mixed ices were studied by Wu et al.,¹⁹ who reported the reaction of a significant amount of the mixture only when the irradiation was performed with extremely short wavelengths (30–60 nm). Very small amounts of CO₂, CO, and methane were unambiguously detected, whereas the presence of other products such as ethane, ethylic alcohol, and formaldehyde was suggested.

5. Concluding Remarks

The photoinduced reactivity by near-UV (350 nm) laser light of mixtures of four different small hydrocarbons (ethane, ethylene, propene, and acetylene) with water has been studied by FTIR and Raman spectroscopy at pressures lower than 1 GPa. The active role of water in triggering the photochemical reaction, recently evidenced in ref 14, is nicely confirmed by this study, even though each mixture presents a peculiar

reactivity accounting for the individual hydrocarbon instability under pressure. With the exception of ethylene, which shows exactly the same behavior in the pure system and in the water mixture, all the other hydrocarbons react differently once mixed with water. In the case of propene, despite the instability threshold pressure and the products of the reaction being quite similar in the pure system and in the water mixture, the CO₂ formation and the coloration of the recovered material, the latter indicating the presence of conjugation, attest to the participation of water in the chemical reaction. The differences are even more pronounced in the ethane and acetylene water mixtures. In fact, both of these species are photochemically stable at the pressure conditions where they react in water mixtures. The extent of the reaction changes completely in the acetylene/water and ethane/water mixtures, reflecting the different molecular instability. Only a small amount of ethane reacts to give CO₂, whereas a massive and more complex reactivity characterizes the acetylene water mixture with the formation of small aliphatic esters. As already reported in low-temperature photoreactions of mixed ices⁵⁰ and in the recent high-pressure photoreactions of nitrogen and CO water mixtures,¹⁴ the products suggest the reaction to be driven by the hydroxyl radicals produced by the two-photon-induced photodissociation of water.

A remarkable result of this study is the identification of a CO₂ clathrate hydrate among the reaction products when the reaction takes place in an excess of water. This clathrate is reported to be stable at moderate pressures also above 0 °C.^{51,52} Therefore, this kind of reactions offers the possibility to perform the in situ sequestration of the carbon dioxide produced during the reactive process. Since CO₂ is a common product when carbon compounds react in these conditions, this result can be very important from an applicative point of view to set up a synthetic method where we can efficiently trap in the same reaction environment this greenhouse gas for further stocking or employment.

In conclusion, several features of the photoinduced high-pressure reactions presented here can be of interest for setting up low-impact new synthetic processes. Near-UV light and moderate pressure are the tools employed to trigger chemical reactions between hydrocarbons and water by using the hydroxyl radicals generated by the photodissociation of water. Solvents, catalysts, and radical initiators are completely missing in these processes, and potentially pollutant products, like CO₂, can be sequestered in the reaction environment for subsequent processing. The mild pressure conditions required for these reactions allow also a potential rapid extension of these processes to large-volume apparatuses.

Acknowledgment. Supported by the European Union under Contract RII3-CT2003-506350, by the Italian Ministero dell'Università e della Ricerca Scientifica e Tecnologica (MURST) and by "Firenze Hydrolab" through a grant by Ente Cassa di Risparmio di Firenze. We thank David Chelazzi for the IR measurements relative to the acetylene/water mixture.

References and Notes

- (1) Schettino, V.; Bini, R.; Ceppatelli, M.; Ciabini, L.; Citroni, M. Chemical Reactions at Very High Pressure. In *Advances in Chemical Physics*; Rice, S. A., Ed.; Wiley: New York, 2005; Vol. 131 pp 105–242.
- (2) Aoki, K.; Usuba, S.; Yoshida, M.; Kakudate, Y.; Tanaka, K.; Fujiwara, S. *J. Chem. Phys.* **1988**, *89*, 529.
- (3) Ceppatelli, M.; Santoro, M.; Bini, R.; Schettino, V. *J. Chem. Phys.* **2000**, *113*, 5991.
- (4) Yoo, C. S.; Nicol, M. *J. Phys. Chem.* **1986**, *90*, 6732.

- (5) Citroni, M.; Ceppatelli, M.; Bini, R.; Schettino, V. *Science* **2002**, 295, 2058.
- (6) Chelazzi, D.; Ceppatelli, M.; Santoro, M.; Bini, R.; Schettino, V. *Nat. Mater.* **2004**, 3, 470.
- (7) Goncharov, A. F.; Gregoryanz, E.; Mao, H. K.; Liu, Z. X.; Hemley, R. J. *Phys. Rev. Lett.* **2000**, 85, 1262.
- (8) Eremets, M. L.; Hemley, R. J.; Mao, H. K.; Gregoryanz, E. *Nature* **2001**, 411, 170.
- (9) Eremets, M. L.; Gavriluk, A. G.; Trojan, I. A.; Dzivenko, D. A.; Boehler, R. *Nat. Mater.* **2004**, 3, 558.
- (10) Iota, V.; Yoo, C. S.; Cynn, H. *Science* **1999**, 283, 1510.
- (11) Santoro, M.; Gorelli, F. A.; Bini, R.; Ruocco, G.; Scandolo, S.; Crichton, W. A. *Nature* **2006**, 441, 857.
- (12) Citroni, M.; Bini, R.; Foggi, P.; Schettino, V. *Proc. Natl. Acad. Sci. U.S.A.* **2008**, 105, 7658.
- (13) Bini, R. *Acc. Chem. Res.* **2004**, 37, 95.
- (14) Ceppatelli, M.; Bini, R.; Schettino, V. *Proc. Natl. Acad. Sci. U.S.A.* **2009**, 106, 11454.
- (15) Nisini, B. *Science* **2000**, 290, 1513.
- (16) Miller, S. L.; Urey, H. C. *Science* **1959**, 130, 245.
- (17) Bar-Nun, A.; Dimitrov, V. *Icarus* **2006**, 181, 320.
- (18) Watanabe, N.; Nagaoka, A.; Shiraki, T.; Kouchi, A. *Astrophys. J.* **2004**, 616, 638.
- (19) Wu, C. Y. R.; Judge, D. L.; Cheng, B.-M.; Shih, W.-H.; Yih, T.-S.; Ip, W. H. *Icarus* **2002**, 156, 456.
- (20) Sokolov, U.; Stein, G. *J. Chem. Phys.* **1966**, 44, 3329.
- (21) Wang, C. C.; Davis, L. L., Jr. *J. Chem. Phys.* **1974**, 62, 53.
- (22) Sloan, E. D.; Koh, C. *Clathrate Hydrates of Natural Gases*, 3rd ed.; CRC Press Taylor & Francis Group: Boca Raton, FL, 2007.
- (23) Chelazzi, D.; Ceppatelli, M.; Santoro, M.; Bini, R.; Schettino, V. *J. Phys. Chem. B* **2005**, 109, 21658.
- (24) Wieldraaijer, H.; Schouten, J. A.; Trappeniers, N. J. *High Temp. High Press.* **1983**, 15, 87.
- (25) Citroni, M.; Ceppatelli, M.; Bini, R.; Schettino, V. *J. Chem. Phys.* **2005**, 123, 194510.
- (26) Bini, R.; Ballerini, R.; Pratesi, G.; Jodl, H. J. *Rev. Sci. Instrum.* **1997**, 68, 3154.
- (27) Gorelli, F. A.; Santoro, M.; Ulivi, L.; Bini, R. *Phys. Rev. Lett.* **1999**, 83, 4093.
- (28) Williams, F.; Varma, S. P.; Hillenius, S. *J. Chem. Phys.* **1976**, 64, 1549.
- (29) Mota, R.; Parafita, R.; Giuliani, A.; Hubin-Franskin, M. J.; Lourenço, J. M. C.; Garcia, G.; Hoffmann, S. V.; Mason, N. J.; Ribeiro, P. A.; Raposo, M.; Liao-Vieira, P. *Chem. Phys. Lett.* **2005**, 416, 152.
- (30) Andresen, P.; Schinke, R. In *Molecular Photodissociation Dynamics*; Ashfold, M. N. R., Baggott, J. E., Eds.; Royal Society of Chemistry: London, 1987; Chapter 3.
- (31) Harich, S. A.; Hwang, D. W. H.; Yang, X.; Lin, J. J.; Yang, X.; Dixon, R. N. *J. Chem. Phys.* **2000**, 113, 10073.
- (32) Thomsen, C. L.; Madsen, D.; Keiding, S. R.; Thogersen, J.; Christiansen, O. *J. Chem. Phys.* **1999**, 110, 3453.
- (33) Kurnosov, A. V.; Ogienko, A. G.; Goryainov, S. V.; Larionov, E. G.; Manakov, A. Y.; Lihacheva, A. Y.; Aladko, E. Y.; Zhurko, F. V.; Voronin, V. I.; Berger, I. F.; Ancharov, A. I. *J. Phys. Chem. B* **2006**, 110, 21788.
- (34) Fleyfel, F.; Devlin, J. P. *J. Phys. Chem.* **1991**, 95, 3811.
- (35) Kumar, R.; Lang, S.; Englezos, P.; Ripmeester, J. *J. Phys. Chem. A* **2009**, 113, 6308.
- (36) Prasad, P. S. R.; Shiva Prasad, K.; Thakur, N. K. *Curr. Sci. India* **2006**, 90, 1544.
- (37) Cardini, G.; Schettino, V.; Klein, M. L. *J. Chem. Phys.* **1989**, 90, 4441.
- (38) Barnes, J. A.; Gough, T. E. *J. Chem. Phys.* **1987**, 86, 6012.
- (39) Mugnai, M.; Cardini, G.; Schettino, V. *J. Chem. Phys.* **2004**, 120, 5327.
- (40) Citroni, M.; Ceppatelli, M.; Bini, R.; Schettino, V. *J. Chem. Phys.* **2003**, 118, 1815.
- (41) Ciabini, L.; Santoro, M.; Gorelli, F. A.; Bini, R.; Schettino, V.; Ragei, S. *Nat. Mater.* **2007**, 6, 39.
- (42) Sakashita, M.; Yamawaki, H.; Aoki, K. *J. Phys. Chem.* **1996**, 100, 9943.
- (43) Brillante, A.; Hanfland, M.; Syassen, K.; Hocker, J. *Physica* **1986**, 139–140, 533.
- (44) Le Sar, R. *J. Chem. Phys.* **1987**, 86, 1485.
- (45) Bernasconi, M.; Chiarotti, G. L.; Focher, P.; Parrinello, M.; Tosatti, E. *Phys. Rev. Lett.* **1997**, 78, 2008.
- (46) Aoki, K.; Kakudate, Y.; Usuba, S.; Yoshida, M.; Tanaka, K.; Fujiwara, S. *J. Chem. Phys.* **1988**, 88, 4565.
- (47) Consani, K.; Pimentel, G. C. *J. Phys. Chem.* **1987**, 91, 289.
- (48) Kirchner, M. T.; Boese, R.; Billups, W. E.; Norman, L. R. *J. Am. Chem. Soc.* **2004**, 126, 9407.
- (49) Lin-Vien, D.; Colthup, N. B.; Fateley, W. G.; Grasselli, J. G. *The Handbook of Infrared and Raman Characteristic Frequencies of Organic Molecules*; Academic Press, Inc: San Diego, 1991.
- (50) Watanabe, N.; Kouchi, A. *Astrophys. J.* **2002**, 567, 651.
- (51) Miller, S. L. *Proc. Natl. Acad. Sci. U.S.A.* **1961**, 47, 1798.
- (52) Ikeda, T.; Mae, S.; Uchida, T. *J. Chem. Phys.* **1998**, 108, 1352.